

A GATED BEAM-POSITION MONITOR AND ITS APPLICATION TO BEAM DYNAMICS MEASUREMENTS AT KEKB

T. Ieiri, H. Fukuma, Y. Funakoshi, K. Ohmi and M. Tobiyama, KEK, Ibaraki, Japan

Abstract

KEKB has transformed to an effective head-on collision by using of crab cavities from a crossing collision and gained a higher specific luminosity. A gated beam-position monitor, being capable of measuring the beam phase as well as the transverse position of a specific bunch in a bunch train, has been developed and is used to measure a beam-beam kick. The monitor estimated the effective horizontal beam size at the interaction point from a linear part of a beam-beam kick and demonstrated the effect of the crab cavities. The estimated horizontal beam size agreed with calculated size considering the dynamic beam-beam effect. Moreover, the monitor detected a displacement of the horizontal beam position along a bunch train under the crabbing collision.

INTRODUCTION

KEKB [1] is a multi-bunch, high-current, electron/positron collider for B meson physics. The collider consists of two storage rings: the Low Energy Ring (LER) for a 3.5-GeV positron beam and the High Energy Ring (HER) for 8-GeV electrons. Both rings store more than 1500 bunches, where the harmonic number is 5120 with an RF frequency of 509 MHz. Bunches are stored in two rings with a 3-bucket (6 ns) or 4-bucket (8 ns) spacing, forming a single bunch train followed by empty buckets that occupies about 5 percents of the circumference. Additional bunches, called pilot bunches, are placed just after the train, at different location in each ring so that they do not collide with each other.

The two beams collide at one interaction point (IP) with a horizontal crossing angle of 22 mrad. Crab cavities installed in 2007 can horizontally tilt a bunch without changing a central orbit using a dipole-mode kick operating at the RF frequency [2]. The crab cavities achieved an effective head-on collision at the IP. The crabbing collisions are successfully performed for the first time and increased a specific luminosity [3]. Since only one crab cavity per ring is installed, the effect of the crab kick could be observed in the whole ring.

The beam-beam effects are important issues from the viewpoint of beam dynamics, including the collision tunings to raise the luminosity. Since the beam-beam force depends on bunch-by-bunch parameters, a bunch-by-bunch measurement is required to study the beam-beam effect. Although a streak camera and an oscilloscope are useful tools to observe a bunch structure, it is not easy to handle them in the usual operations. Moreover, a direct measurement of the beams at the IP is difficult in the actual configurations. On the other hand, a gated beam-position monitor, being capable of measuring the beam phase as well as the transverse position of a

specific bunch in a bunch train, is a simple tool to measure a beam-beam kick. The beam-beam kick can be measured by comparing a beam position between colliding and non-colliding bunches. Although a part of a gated beam-position monitor has already been reported [4], this note represents revised performances and new applications to beam dynamics measurements under the crabbing collision.

GATED BEAM-POSITION MONITOR

A gated beam-position monitor (GBPM), a fast switch selecting a specific bunch is attached with a turn-by-turn BPM, can measure the beam position of individual bunches. One application of a GBPM is to measure the beam-beam effect by comparing the beam parameters of a colliding bunch with those of the non-colliding pilot bunch. The signal processing is performed within a revolution period. This gated measurement has the following features:

- The position measurement is not affected by the global orbit correction.
- Imbalance in gains of the detector is cancelled out due to subtraction.
- However, the measurement is not simultaneous.
- An error would be enhanced, when the intensity between bunches to be measured is largely unbalanced.

Figure 1 shows the schematic diagram for a GBPM. Button type electrodes are mounted with a cylindrical vacuum pipe with a diameter of 64 mm to pick up a beam pulse. The optics parameters at the location of the pickups are listed in Table 1. The system can select an electron or a positron bunch and employs a common detector. A low-pass filter of a Bessel type with a cut-off frequency of 1.5 GHz is attached to a gate module so that high frequency components of a button signal would be eliminated. A gate selects a specific bunch in a bunch train with a pulse width of 8 ns, where a commercially available switch (Hittite-HMC234C8) is used. Owing to the IQ (In-phase and Quadrature phase) detection at the acceleration frequency of 509 MHz, the monitor can detect a longitudinal position or the beam phase of a bunch as well as the transverse beam positions [5]. Two orthogonal signals are put into 8-channel ADCs with a resolution of 12 bits. A peak of a detected pulse with 20 ns width is sampled in the ADCs at a rate of the revolution frequency of 100 kHz. The sampled data are stored turn by turn in a memory.

An on/off isolation of the gate module was tested in a bench. An isolation of more than 50 dB at 2 GHz is achieved, where two series of the switches are used to raise the isolation. The isolation of the system was also measured using real bunches placed with a spacing of 8

ns (4 buckets), while shifting the timing for the gate and for the clock of the ADCs in the unit of bucket. The isolation for the beam intensity was about 40 dB at a separation of 3 buckets as shown in Fig. 2. The degradation in the isolation would be due to a long tail of a button signal. Although the system can measure a beam position turn by turn, the beam position data are averaged over 2,000 turns for measuring a closed orbit. The standard deviation of the averaged position measurement was improved to 3 to 5 μm and the resolution of the phase is 0.10 degrees. The performances of the GBPM are summarized in Table 2.

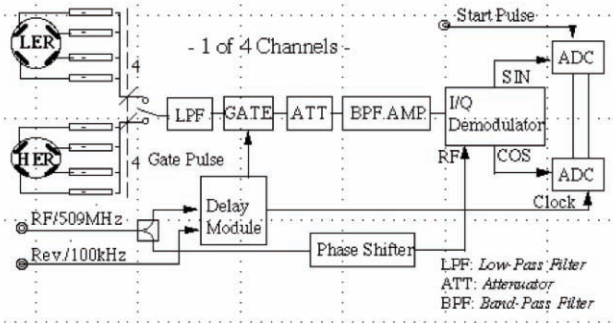


Figure 1: Schematic diagram of a gated beam-position monitor system.

Table 1: Optics parameters at GBPM

Ring	LER	HER
Location	QV1P.2	QX6E.2
Beta _x (m)	22.4	43.05
Betatron Phase	22.68	23.31
Advance /2 π from IP		
Dispersion _x (m)	< 0.0001	0.001

Table 2: Specifications of GBPM

Pick-up Electrode	Button
Detector Bandwidth	509+/- 30 MHz
Resolution of Position	20 μm @ turn-by-turn 3 to 5 μm @ average
Resolution of Phase	0.3 deg. @ turn-by-turn 0.10 deg. @ average
Isolation of Gate	> 50 dB @ 2GHz 40 dB @ 6 ns spacing

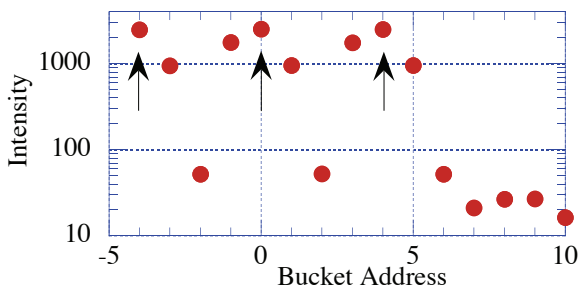


Figure 2: Measured intensity of positron bunches, while shifting timing for the gate and the sampling clock as a

function of bucket address. Arrows indicate buckets with a bunch and the other buckets do not contain bunches.

BEAM-BEAM KICK

When two beams collide with an orbit offset, Δx^* at the IP, they are kicked by the electromagnetic force of the opposite beam and the orbits of both beams are distorted around the ring. A position monitor located at a phase advance of $\Delta\varphi_d$ from the IP detects a position shift due to the collision. A position shift at a detector is given by

$$\Delta X_{\text{det.}} = \frac{\sqrt{\beta_{\text{det.}} \beta^*}}{2 \sin(\pi\nu)} \theta_{bb} \cos(\pi\nu - |\Delta\varphi_d|). \quad (1)$$

Here, $\beta_{\text{det.}}$ and β^* are the beta functions at a detector and the IP, respectively and ν is the betatron tune and θ_{bb} is a beam-beam kick angle. Assuming that the vertical offset is zero, the horizontal beam-beam kick θ_{bb} is expressed using a rigid Gaussian model as

$$\theta_{bb} = \frac{-2r_e N_b \Delta x^*}{\gamma} \int_0^{\infty} \frac{\exp(-\frac{\Delta x^2}{t + 2\Sigma_x^2})}{(t + 2\Sigma_x^2)^{3/2} (t + 2\Sigma_y^2)^{1/2}} dt, \quad (2)$$

where, Σ_x and Σ_y are horizontal and vertical effective beam sizes, respectively, r_e is the classical electron radius, γ is the relativistic factor, N is the number of particles in a bunch. The effective beam size is defined by $\Sigma_{x/y} = \sqrt{(\sigma_{x/y}^+)^2 + (\sigma_{x/y}^-)^2}$. The superscript \pm denotes positron or electron bunches. The beta function dynamically changes according to the beam-beam force, depending on the betatron tune. A calculation using the optics parameters shows that the product of the beta function is constant to be $\sqrt{\beta_{\text{det.}} \beta^*} \approx 4.0\text{m}$. Thus, the position shift at the detector is proportional to the beam-beam kick. When the horizontal offset is smaller than the beam size, Eq. (2) is approximately given by

$$\theta_{bb}^{\pm} \approx \frac{-1.94 r_e N^{\mp}}{\gamma^{\pm}} \frac{\Delta x^*}{\Sigma_x^2}. \quad (3)$$

We can estimate the effective horizontal beam size at the IP from the slope, $\theta_{bb}^{\pm} / \Delta x^*$ using Eq. (3).

Since the analytical formula in Eq. (2) is based on the head-on collision, a different configuration is required to calculate a beam-beam kick with a crossing angle. Figure 3 illustrates how to calculate the beam-beam kick under collision with a crossing angle of 22 mrad, assuming that a single particle collides with a Gaussian strong bunch. A particle is horizontally moved with a crossing angle. The each kick data are summed up, considering the longitudinal beam profile of the bunch. Figure 4 compares two beam-beam kicks of particles with and without the crossing angle under the same bunch intensity. Transforming the crossing scheme to the head-on collision from the crossing collision, the beam-beam kick is increased and the estimated effective beam size would decrease. Since the slope in a head-on collision around the linear part is roughly twice comparing with a crossing

collision, it is estimated that the relative beam size reduces by a factor of 1.4 due to the crabbing collision.

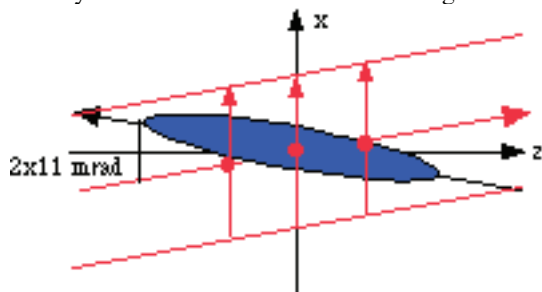


Figure 3: Schematics of calculating a beam-beam kick of a particle under a crossing angle of 22 mrad. The “x” and “z” mean the horizontal and longitudinal directions, respectively. A particle moves in the horizontal direction with a slope of 22 mrad for a bunch.

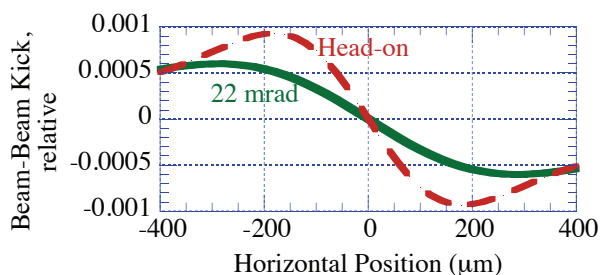


Figure 4: Relative beam-beam kick as a function of the horizontal position, dashed red is that with head-on collision and solid green line is that with a horizontal crossing angle of 22 mrad under the same beam conditions.

MEASUREMENTS

Beam-Beam Kick

Although a tilt of a bunch profile due to the crab cavities is directly observed by using a streak camera [6], its effect would be estimated from measuring a beam-beam kick at the IP, as estimated in the calculation. The GBPM compares a position between colliding and non-colliding bunches, while changing a relative orbit between the electron and the positron beams at the IP. After careful tuning of the crab voltage and the phase, the horizontal orbit scan was performed at the IP. Figure 5 shows the position shift with and without the crab cavity as a function of a setting value of the horizontal offset. It was confirmed that the horizontal offset agreed with the actual orbit displacement at IP within 10%. Both beam-beam kicks were taken under almost the same beam conditions except the crab voltage. There is a clear difference in the slope around the zero offset between two conditions. The estimated effective horizontal beam size using Eq. (3) is $\Sigma_x = 167 \pm 3 \mu\text{m}$ with the crab voltage and $\Sigma_x = 230 \pm 3 \mu\text{m}$ without the crab. The horizontal effective size at the IP reduced to 72 % by the crabbing collision. The measurement is consistent with the calculation. The reduction of the horizontal beam size could contribute an increase of the luminosity. Since the crab cavity is so

effective, the operations are performed under the crabbing collision. The effective beam size was measured in the usual operations. The measured beam size was smaller than a calculated size without the beam-beam force as shown in Fig. 6. Since the horizontal betatron tune is close to a half-integer, the dynamic beam-beam effect greatly contributes to the beam size. Figure 6 shows that the dynamic effect with betatron tune of 0.51 or 0.54 can explain the measured beam size.

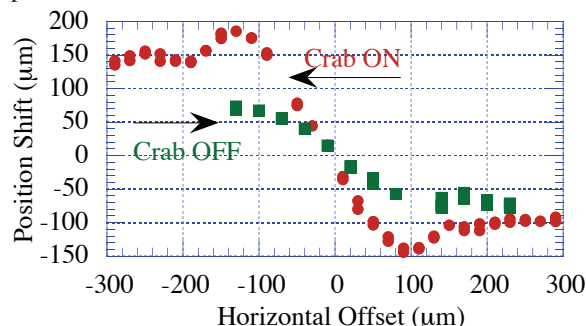


Figure 5: The position shift of a positron bunch detected at the monitor as a function of the horizontal orbit offset, red dots are measured under the crabbing collision and green squares are without the crab. The positron and electron bunch currents are 0.64 and 0.47 mA with the crab, 0.73 and 0.42 mA without the crab, respectively.

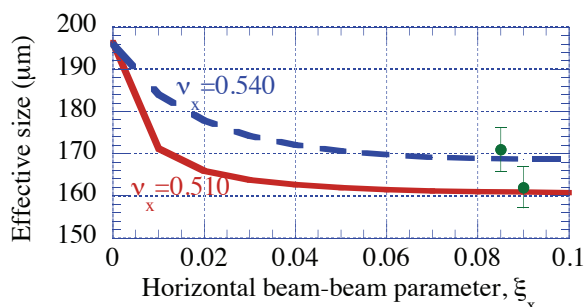


Figure 6: Measured effective horizontal beam size indicated with green dots as a function of the beam-beam parameter. The beam-beam parameter was estimated from a coherent beam-beam tune shift. Calculated sizes are shown in the case of two fractional tunes, 0.510 with a solid red line and 0.540 with a blue dashed line.

Beam Positions along a Bunch Train

The beam position and the beam phase along a bunch train were measured every 49 buckets using averaged data under the crabbing collision, where a bunch train contains 1584 bunches. Figure 7 shows the horizontal position, the vertical position and the beam phase as a function of the bucket number, measured in the LER. Similar measurements were performed in the HER as shown in Fig. 8. As shown in Fig. 7-(c) and Fig. 8-(c), the beam phase advances along a bunch train. The phase modulation is known as transient beam loading due to the gap after a train [7] and its maximum displacement is proportional to the beam current. Comparing Fig. 7-(c)

with Fig. 8-(c), there is a small difference in the phase advancing. The phase advance in the LER rapidly increases in the leading part and tends to saturate in the backward region. On the other hand, the phase in the HER almost linearly increases along a train. The difference would be due to the RF systems. KEKB employs two types of cavities, normal and superconducting cavities. At the same time, we observed a peculiar phenomenon in the horizontal position, where the position drifts inside along a train in both rings. The horizontal orbit displacement between the head and the tail bunches is about $120\ \mu\text{m}$ in the LER and about $280\ \mu\text{m}$ in the HER. Note that the horizontal dispersion function at the location of the monitor is negligibly small in both rings. Since such a large horizontal displacement was not observed without the crab cavities, the horizontal displacement might be related to the crab kick. The vertical position did not show a peculiar displacement, except in the leading part in the LER.

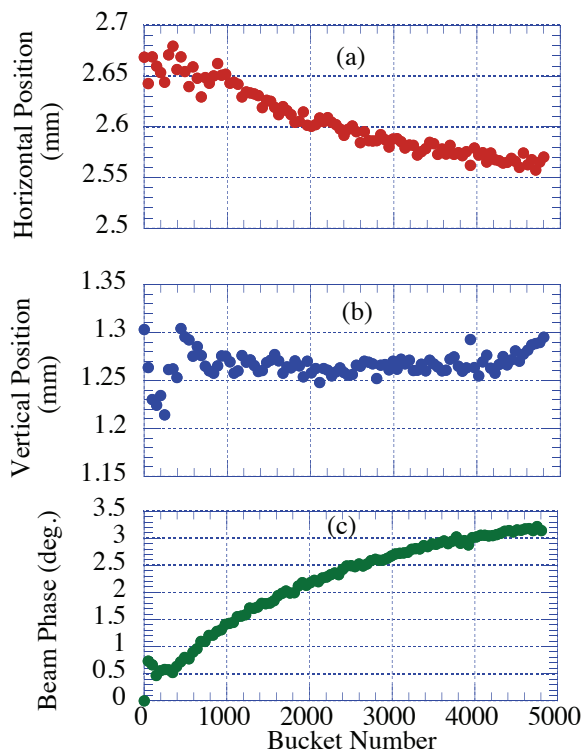


Figure 7: The horizontal beam position (a), the vertical position (b) and the beam phase (c) along a train in the LER measured at beam current of 1530 mA.

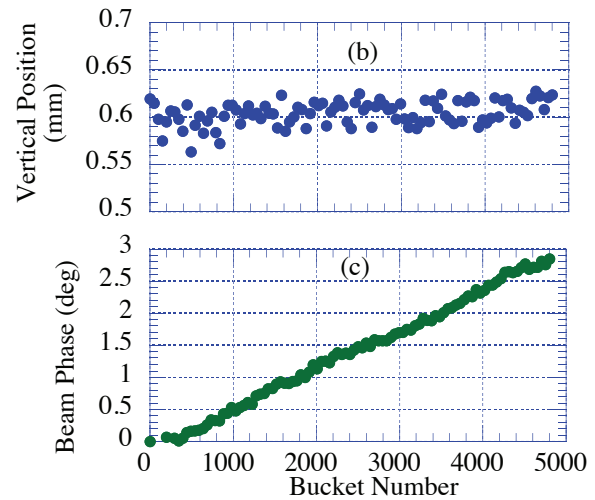
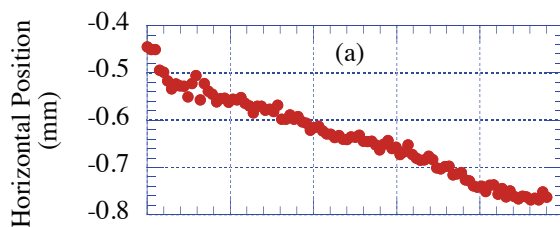


Figure 8: The horizontal beam position (a), the vertical position (b) and the beam phase (c) along a train in the HER measured at beam current of 800 mA.

Detail structure of the position along a train was measured. A bunch train has a periodic structure with a period of 49 buckets. Each period contains 16 bunches. In a period, only one bunch is placed with 4-bucket spacing and the others are placed with 3-bucket spacing. As shown in Fig. 9, we observed orbit displacements of about $60\ \mu\text{m}$ in the horizontal and the vertical positions just before the 4-bucket spacing. The displacement in the vertical position reduced, when the beam current decreased.

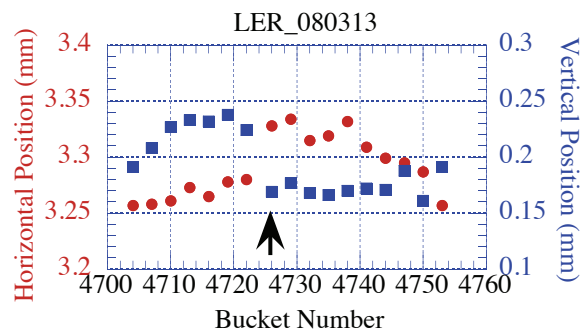


Figure 9: The horizontal (red dots) and the vertical positions (blue squares) as a function of bucket number, measured at total beam current of 1600 mA in the LER. Only one bunch indicating an arrow is placed with 4-bucket spacing. The others are placed with 3-bucket spacing.

DISCUSSION

The beam-beam kick angle can be obtained from the position shift data using the optics parameters. A measured beam-beam kick is represented together with calculated kicks as shown in Fig. 10. The measured kick agrees well with a calculated kick around the center, assuming a rigid Gaussian bunch with an effective size of $162\ \mu\text{m}$. However, the measured kick deviates from the calculated kick curve, when the horizontal offset is larger than about $100\ \mu\text{m}$. The measured kick is smaller than a

calculated one using a larger size of $196 \mu\text{m}$ there. The result suggests that a beam density at the peripheral region of a bunch profile reduces and somewhat expands, although the central part is shrunk by the dynamic beam-beam effect. The distorted horizontal profile might be related to a short lifetime observed at a high beam-beam parameter.

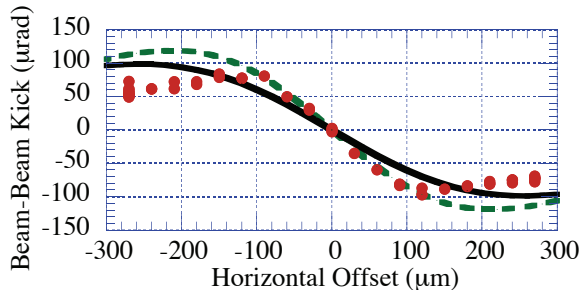


Figure 10: Measured (red dots) and calculated (dashed green and solid black) beam-beam kick as a function of the horizontal offset. The dashed green line indicates a kick with an effective size of $162 \mu\text{m}$ and the solid black with a size of $196 \mu\text{m}$ with a Gaussian profile.

As shown in Figs. 7 and 8, we observed the horizontal displacement as well as the beam-phase advance along a train in both beams. When a bunch shifting the synchronous phase passes through a crab cavity, the crab cavity kicks the bunch asymmetrically. As a result, a horizontal orbit displacement would be produced in the whole ring. The position-monitor detects the displacement as

$$\Delta X_{\text{det.}} = \frac{\sqrt{\beta_{\text{det.}} \beta_c}}{2 \sin(\pi\nu)} \Delta\phi_{\text{crab}} \cos(\pi\nu - |\Delta\varphi_d|), \quad (4)$$

where β_c , $\Delta\phi_{\text{crab}}$, $\Delta\varphi_d$ are the beta function at the crab cavity, an asymmetric kick angle of the crab cavity and a betatron phase advance between the crab and the monitor, respectively. It is experimentally verified that a crab kick for a phase displacement of $4.8 \mu\text{rad/deg}$ is produced at crab voltage of 1 MV in the LER [8]. On the other hand, the phase amount in a train is measured to be about 3.2 degrees from Fig. 7-(a), which makes a position shift of $140 \mu\text{m}$ between the head and the tail bunches in a train. The estimated position shift agrees well with the measurement.

As shown in Fig. 9, position displacements were observed around changing the bunch spacing. In order to search the source, we tried to measure the beam position directly using an oscilloscope (Tektronix, DPO7254). Figure 11 shows a bunch signal picked up by a button electrode through a coaxial cable. A ringing is observed after a button signal with frequencies of 2 to 3 GHz. A large vertical position displacement was observed from a peak-to-peak measurement in the button signal, however, the displacement was reduced by using a low-pass filter with a cut-off frequency of 1.5 GHz. The ringing would be due to wake fields detected by button electrodes. It was confirmed that the low-pass filter attached to the gate

module is effective to attenuate unnecessary high frequency components.

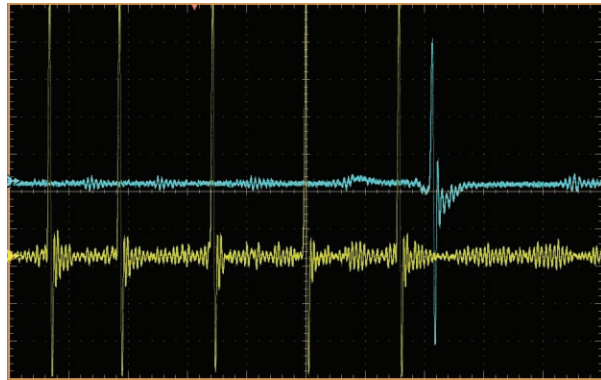


Figure 11: Button signals observed on an oscilloscope. Yellow trace is a bunch signal and upper blue one is a gated bunch signal. The horizontal scale is 5 ns /div.

SUMMARY

Under the crabbing collision, the beam-beam kick and the beam position along a bunch train were measured using a gated beam-position monitor at KEKB.

- The effect of the crab cavity was confirmed from measuring the effective horizontal beam size at the IP.
- The measured horizontal beam size at the IP is consistent with calculation with the dynamic beam-beam effect.
- However, the kick data suggest that a bunch profile deviates from a Gaussian in the peripheral region.
- Displacements of both the horizontal position and the beam phase were observed along a bunch train. The horizontal-position displacement is caused by an asymmetric kick of the crab cavity, which is based on the transient beam loading.
- Displacements in the horizontal and the vertical positions were observed around a change of bunch spacing. The source is still unclear and the displacements might not be real.

REFERENCES

- [1] K. Akai et al., Nucl. Instrum. Methods Phys. Res., Sect. A 499, p.191 (2003).
- [2] K. Hosoyama et al., to be presented in EPAC08, (2008).
- [3] K. Oide et al., Proc. of PAC07, p.27 (2007).
- [4] M. Arinaga et al., Nucl. Instrum. Methods Phys. Res., Sect. A 499, 100 (2003).
- [5] T. Ieiri and T. Kawamoto, Nucl. Instrum. Methods Phys. Res., Sect. A 440, p.330 (2000).
- [6] H. Ikeda et al., Proc. of PAC07, p.4018 (2007).
- [7] K. Akai et al., Proc. of PAC01, p.2432 (2001).
- [8] H. Koiso, Private communications.